

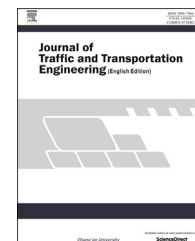
HOSTED BY



ELSEVIER

Available online at www.sciencedirect.com

ScienceDirect

journal homepage: www.elsevier.com/locate/jtte

Original Research Paper

Characterization of pavement texture by means of height difference correlation and relation to wet skid resistance



Stefan Torbruegge*, Burkhard Wies

Continental Reifen Deutschland GmbH, Hannover 30419, Germany

ARTICLE INFO

Article history:

Available online 21 February 2015

Keywords:

Pavement texture
Friction
Rubber
Height difference
Skid resistance

ABSTRACT

Driving safety is of utmost importance in the automobile industry and is acknowledged by the introduction of the tire wet grip index as part of the EU tire label. The rubber pavement interaction is determined by the viscoelastic properties of the rubber as well as by the pavement texture. Nowadays available optical surface profiling instruments allow for a detailed measurement of surface roughness covering several length scales. This enables the validation of a mathematical statistical description of pavement texture within the framework of self-affine surfaces and hence provides a holistic characterization of surface roughness covering several length scales within a few characteristic parameters.

We deduce within this article the correlation between classical surface roughness parameters and the parameter set of self-affine surfaces. These parameters allow for a detailed understanding of the relationship between pavement texture and its wet skid resistance. We present wet skid resistance measurements with the British pendulum and a linear friction tester device on different pavement textures. We demonstrate that the so-called estimated texture depth does not correlate to the surface skid resistance measured with the British pendulum. Finally, we deduce a dependency of wet skid resistance on pavement texture which is supported by current models for hysteresis friction.

© 2015 Periodical Offices of Chang'an University. Production and hosting by Elsevier B.V. on behalf of Owner. This is an open access article under the CC BY-NC-ND license (<http://creativecommons.org/licenses/by-nc-nd/4.0/>).

1. Introduction

The quantitative evaluation of surface roughness is of major interest in various industrial applications. The study of road surface texture is of great importance in pavement engineering as it determines among other factors the noise emission

from the tire-pavement interface, the frictional forces that can be transmitted between tire and pavement and the water drainage capacity (ISO 13473-1: 1997, 1997). Typically these different applications require studies of the pavement texture at specific characteristic length scales relevant for the application. The challenge in studying the relationship between the pavement wet skid resistance and its texture

* Corresponding author. Tel.: +49 51197634164.

E-mail addresses: stefan.torbruegge@conti.de (S. Torbruegge), Burkhard.wies@conti.de (B. Wies).

Peer review under responsibility of Periodical Offices of Chang'an University.
<http://dx.doi.org/10.1016/j.jtte.2015.02.001>

2095-7564/© 2015 Periodical Offices of Chang'an University. Production and hosting by Elsevier B.V. on behalf of Owner. This is an open access article under the CC BY-NC-ND license (<http://creativecommons.org/licenses/by-nc-nd/4.0/>).

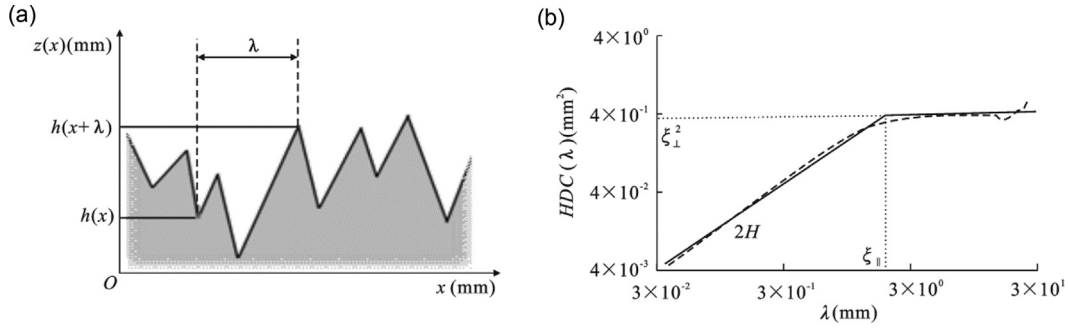


Fig. 1 – Height difference at a given λ and its relationship with ξ_{\parallel} , ξ_{\perp}^2 and H (Solid line indicates a least squares fit of Eqs. (3) and (4) to $HDC(\lambda)$). (a) Schematic height profile $z(x)$ highlighting the height difference for a given lateral length scale λ . (b) Height-difference correlation function with three characteristic parameters ξ_{\parallel} , ξ_{\perp}^2 and H .

lies in the roughness characterization for all length scales possibly from centimeter to micrometer. Another challenge lies within the measurement of wet skid resistance. As friction always depends on both contact partners which are sliding with respect to each other (in our case a piece of rubber or tire and the pavement surface), there exists not a unique friction coefficient for a given surface but it depends on the instrument that has been used for the measurement. A friction coefficient measured on a given pavement texture always depends on the rubber properties and in addition also on the measuring conditions (contact pressure, velocity and temperature). Hence, it is obvious that these conditions need to be accounted when the relationship between pavement texture and its wet skid resistance is studied.

2. Statistical description of pavement texture

Recently it has been suggested to describe the pavement texture within the framework of self-affine surfaces (Klüppel and Heinrich, 2000; Persson, 2001). In the following we will introduce the concept of self-affine surfaces and the resulting surface roughness description for this class of surfaces.

2.1. Texture description for self-affine surfaces

2.1.1. Height-difference correlation function

For a mathematical analysis of the roughness of a surface texture we can assume the height profile $z(x)$ to be self-affine, i.e. for an arbitrary scaling factor A the following transformation property holds true

$$x \rightarrow Ax, \quad z \rightarrow A^H z \quad (1)$$

where H is the so-called Hurst exponent which is related to the fractal dimension D , $D=3-H$, $0 \leq H \leq 1$.

Note that for simplicity in Eq. (1) a two-dimensional notation is used. One possibility for the description of the surface roughness of a self-affine surface is to consider the height-difference correlation function

$$HDC(\lambda) = \langle (z(x+\lambda) - z(x))^2 \rangle_x \quad (2)$$

where $\langle \dots \rangle_x$ denotes averaging over x , $HDC(\lambda)$ describes the mean square height difference of the surface with respect to the horizontal length scale λ .

Fig. 1(a) displays schematically a height profile with the height difference between two points indicated. In the case of a self-affine height profile $z(x)$, the height-difference correlation function can be written as

$$HDC(\lambda) = \left(\frac{\lambda}{\xi_{\parallel}} \right)^{2H} \xi_{\perp}^2 \quad \text{for } \lambda < \xi_{\parallel} \quad (3)$$

$$HDC(\lambda) = \xi_{\perp}^2 \quad \text{for } \lambda < \xi_{\parallel} \quad (4)$$

Here we have introduced the correlation lengths ξ_{\parallel} in horizontal direction and ξ_{\perp} in vertical direction. The power law in Eqs. (3) and (4) follows directly from the definition in Eq. (1) of self-affinity and can therefore be used as a criterion for the self-affinity of a given surface texture. Note that the height-difference correlation function allows for a roughness characterization covering many length scales λ and that it is uniquely determined by the three roughness parameters H , ξ_{\parallel} and ξ_{\perp}^2 . Fig. 1(b) depicts exemplarily a $HDC(\lambda)$ plot on a double logarithmic scale for a self-affine surface texture with the three roughness parameters indicated.

At small length scales $\lambda < \xi_{\parallel}$, the $HDC(\lambda)$ can be well approximated by the slope from Eq. (3). This implies that the roughness at each length scale λ is increasing in accordance to the slope $2H$ until λ approaches ξ_{\parallel} and the roughness at ξ_{\parallel} then reaches a saturation level ξ_{\perp}^2 . For length scales $\lambda > \xi_{\parallel}$, the surface roughness (or height difference) is not increasing any more with increasing distance λ between two points of the height profile. Roughly speaking, ξ_{\parallel} corresponds to the mean spacing of the aggregates used in an asphalt grading curve and ξ_{\perp} corresponds to their mean height. We will discuss the meaning of the three parameters in more detail in the following section.

2.1.2. Practical meaning of ξ_{\perp} , ξ_{\parallel} and H for surface texture

The HDC comprises several important features for the rigorous description of pavement texture. In Fig. 2(a) and (c) we present two height profiles which have been manipulated numerically. The impacts of these changes on

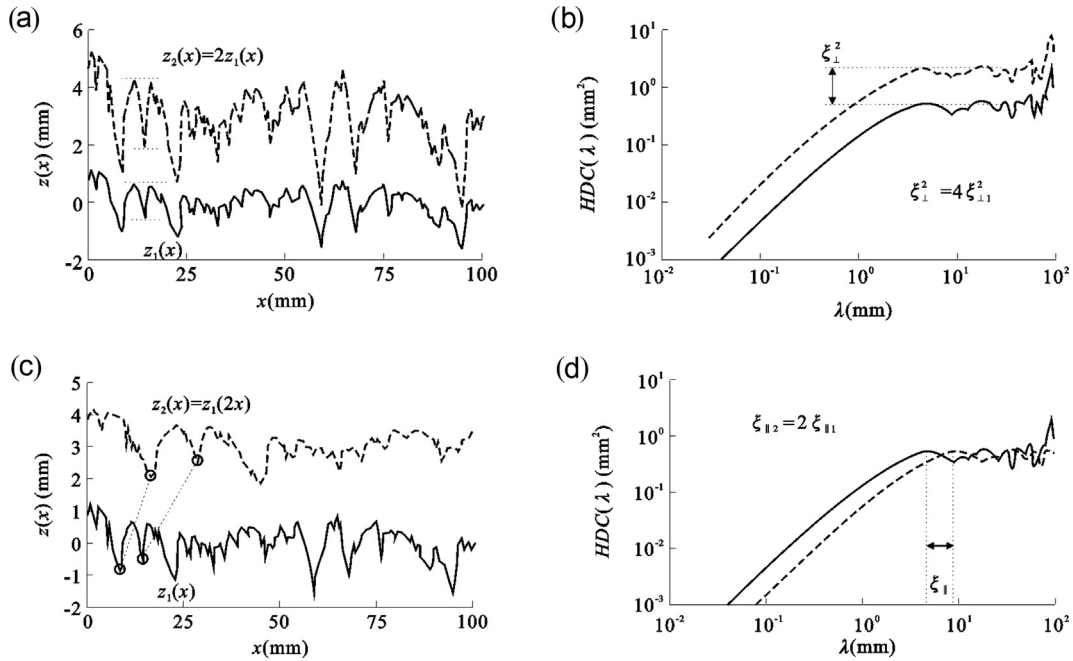


Fig. 2 – Manipulated height profiles and the corresponding HDC plots. (a) Height profile $z_1(x)$ measured an asphalt concrete together with a numerically manipulated height profile $z_2(x) = 2z_1(x)$. (b) Corresponding HDC plots calculated from the height profiles in Fig. 2(a). (c) Height profile $z_1(x)$ measured an asphalt concrete together with a numerically manipulated height profile $z_2(x) = z_1(2x)$. (d) Corresponding HDC plots calculated from the height profiles in Fig. 2(c).

HDC are displayed in Fig. 2(b) and (d), respectively. In Fig. 2(a), for better readability $z_2(x)$ was shifted along the z -axis. Please note that this does not affect the HDC evaluation since here only relative height differences are calculated.

In Fig. 2(a) the second height profile $z_2(x)$ has been constructed from $z_1(x)$ by scaling with a factor of 2 in order to increase its amplitude at all length scales λ . This is for example a simplification of removal of bitumen captured between the stones of an asphalt concrete pavement. This scaling leads to a vertical shift of $HDC_2(\lambda)$ in comparison to $HDC_1(\lambda)$ with an increased ξ_{\perp}^2 value of $\xi_{\perp 2}^2 = 4\xi_{\perp 1}^2$ (Fig. 2(b)). This shift can be proven mathematically by the following calculation

$$\begin{aligned} HDC_2(\lambda) &= \langle (z_2(x+\lambda) - z_2(x))^2 \rangle_x \\ &= \langle (2z_1(x+\lambda) - 2z_1(x))^2 \rangle_x \\ &= 4 \langle (z_1(x+\lambda) - z_1(x))^2 \rangle_x \\ &= 4HDC_1(\lambda) \end{aligned} \quad (5)$$

Please note that the slope H (and hence the fractal dimension) as well as the lateral correlation length ξ_{\parallel} are unchanged while solely the HDC is shifted vertically. This is in excellent agreement with the result of Russ (1994).

In the second example we demonstrate the meaning of ξ_{\parallel} . In Fig. 2(c) the initial height profile is identical to $z_1(x)$ in Fig. 2(a). Now $z_2(x)$ has been created by the numerical operation $z_2(x) = z_1(2x)$. This leads to a stretching of the height profile along the x -axis. Practically such an effect may be achieved for example by a shift of the grading curve of the asphalt recipe to larger grain sizes which

implies a bigger spacing between the stones. The stretching of $z_2(x)$ becomes visible in the calculated HDC curves in Fig. 2(d) by a horizontal shift of $HDC_2(\lambda)$ and consequently an increase of $\xi_{\parallel 2} = 2\xi_{\parallel 1}$. In other words, due to the lateral stretching of the roughness profile also a larger length scale λ needs to be covered until the asymptotic roughness ξ_{\perp}^2 is achieved.

2.1.3. Statistical derivation of ξ_{\perp}

The correlation length ξ_{\perp} normal to the surface is closely related to the variance Var of the measured height distribution of a surface profile. The variance is calculated by

$$Var(z) = \langle z(x) - \langle z \rangle \rangle^2 \quad (6)$$

where $\langle z \rangle$ is the mean height of the surface profile. For self-affine surfaces the variance is related to ξ_{\perp} by the following equations (Kluppel and Heinrich, 2000; Russ, 1994)

$$Var(z) = \frac{1}{2} r_{\perp}^2 \quad (7)$$

and consequently

$$\xi_{\perp} = \sqrt{2Var(z)} = \sqrt{2}\sigma_z = \sqrt{2} \sqrt{\langle z^2 \rangle - \langle z \rangle^2} \quad (8)$$

Where σ_z is the mean standard deviation. Note that these mathematically derived Eqs. (7) and (8) were confirmed numerically within our thorough studies of asphalt concrete and porous asphalt surfaces. We will take advantage of this relation in Section 2.3 for the correlation of the mean texture depth (MTD) to ξ_{\perp} .

2.2. Characterization of pavement texture by means of height-difference correlation

In the following, we will demonstrate the feasibility of the height-difference correlation for the characterization of pavement textures typically found on public roads. For this purpose we analyzed optical surface measurements of several road surfaces, namely asphalt concrete and porous asphalt. The height-difference correlation plots for these two pavement textures are displayed exemplarily in Fig. 3 together with the corresponding least squares fits of Eqs. (3) and (4).

The fits of Eqs. (3) and (4) to the HDC curves show a very good agreement for both pavements. Thus it can be concluded that both pavement textures show self-affinity over several length scales. This is in excellent agreement with the reported findings of Klüppel and Heinrich (2000) and Persson (2001).

In next step, we take a closer look to the previously introduced HDC parameters for these two pavement textures. The porous asphalt shows a larger ξ_{\perp} than asphalt concrete. This is due to the less amount of bitumen used in porous asphalt resulting in more exposed stones. Also for ξ_{\parallel} the difference is visible. ξ_{\parallel} of the porous asphalt is larger reflecting the large troughs between the stones due to the less amount of bitumen used and a shift of the grading curve to larger grain sizes for the porous asphalt in comparison to asphalt concrete. While ξ_{\parallel} and ξ_{\perp} reflect more macroscopic shape of the pavement texture, the slope of the HDC curves yields access to the surface roughness also at microscopic scales down to the smallest λ considered. Also for H , a differentiation between the two pavement textures is visible in Fig. 3. More precisely, the porous asphalt exhibits a smaller slope H compared to the asphalt concrete due to larger roughness (or height difference) at all length scales $\lambda < \xi_{\parallel}$.

2.3. Relation between height difference correlation and estimated texture depth

In pavement engineering the so-called ‘sand-patch’ method, or the more general ‘volumetric patch’ method (ASTM Standard E965-96, 2006) has been used worldwide for many years to give a very simple measurement describing the surface macro texture (ISO 13473-1: 1997, 1997). Along with developments in contactless surface profiling techniques

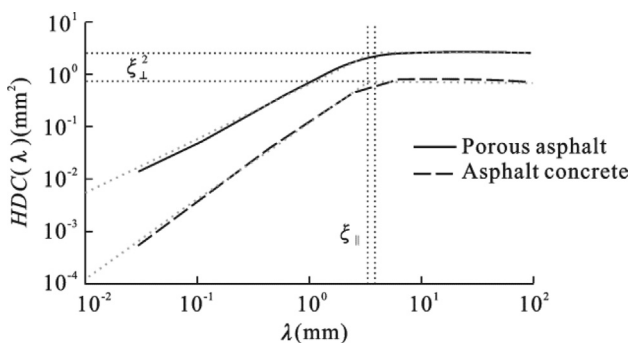


Fig. 3 – HDC(λ) plots for porous asphalt and asphalt concrete pavement (Bold dotted lines indicate least squares fits of Eqs. (3) and (4) to the measured data).

(e.g. laser triangulation setups) it has become possible to replace the sand-patch method with those derived from profile recordings. A test method has been established suitable for determining the mean profile depth (MPD) of a pavement surface (ISO 13473-1: 1997, 1997). This MPD can be transformed to a quantity which estimates the macro texture depth according to the volumetric patch method, the estimated texture depth (ETD). The ETD can be derived from height profile measurements by the following relation

$$\text{ETD} = 0.2 + 0.8 \times \text{MPD} \quad (9)$$

where MPD is estimated from a measured surface height profile $z(x)$ by means of the following equation

$$\text{MPD} = \frac{1}{2} \left(\max_{0 \leq x \leq l} z(x) + \max_{l < x \leq L} z(x) \right) - \langle z \rangle \quad (10)$$

where $\langle z \rangle$ is the average height level, L is the total profile length and $l=L/2$.

Fig. 4 schematically shows how the MPD is derived from a measured height profile. Comparing Eq. (10) with Eq. (8) we observe that MPD definition can be interpreted as a variance-type equation. Note that in opposite to Eq. (8) for the MPD only a single value namely the averaged maximum value of the first and second half of the height profile is considered.

For the practical estimation of the MPD a height profile of minimum length $L=100$ mm is divided into two halves of length l . A possible inclination slope of the profile (due to some tilt between measurement setup and pavement surface) is suppressed by calculation of a regression line and subtraction of this line and additionally high frequency noise is eliminated by appropriate low-pass filtering (ISO 13473-1: 1997, 1997). In Fig. 4 such a processed surface height profile measured on an asphalt concrete surface is shown. The maximum levels of the first and the second half as well as the MPD according to Eq. (10) are indicated. For comparison $\xi_{\perp} = \sqrt{2\text{Var}(z)}$ (Eq. (8)) is also shown.

Since ξ_{\perp} relates directly to the standard deviation σ_z of the measured height values it is straight forward to expect a correlation between MPD (consequently also for the ETD due to the linear relationship in Eq. (8)) and ξ_{\perp} . However, due to the singular evaluation of maximums within each half of a height profile in case of that MPD provides rather poor statistics compared to ξ_{\perp} which reflects the variance of the height distribution of all measured height values.

In Fig. 5(a) we compare the calculated MPD values for an asphalt concrete patch of size 100 mm \times 100 mm. More precisely, from the 3D measurement 850 single height profiles were extracted and MPD and ξ_{\perp} values have been calculated respectively. The height profile comparison of both parameters shows some correlation as presented in Fig. 5(b). Note that for a rather small patch of asphalt concrete we registered a broad range of MPD and ξ_{\perp} values ranging from 0.5 mm to 1.2 mm. In addition we also plotted in Fig. 5(b) the mean values $\langle \text{MPD} \rangle$ and $\langle \xi_{\perp} \rangle$ calculated by averaging over all height profiles displayed in Fig. 5(a). These mean values are based on a larger data set and therefore should result in a better correlation of MPD and ξ_{\perp} due to the increased statistics, especially for MPD.

Due to this observation we measured the surface texture of several areas of 100 mm \times 100 mm on different asphalt

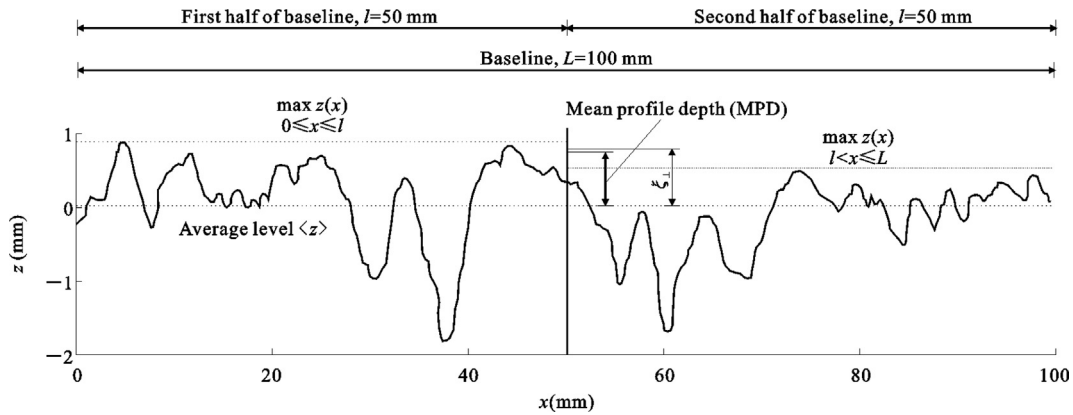


Fig. 4 – Definition of mean profile depth (MPD).

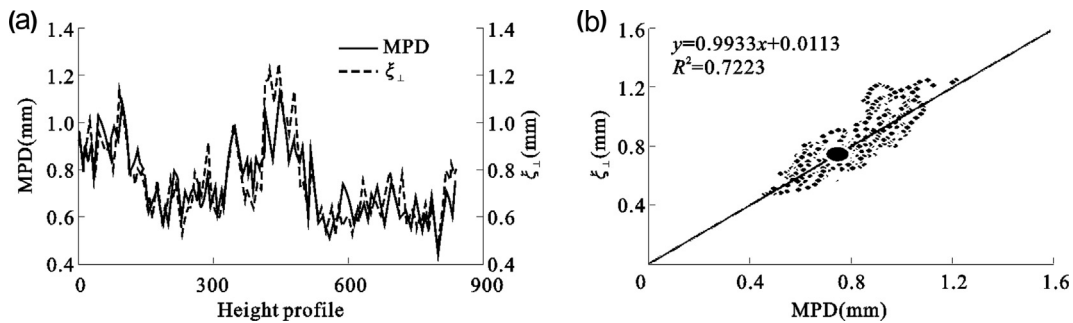


Fig. 5 – Relationship between MPD and ξ_{\perp} . (a) Calculated MPD and ξ_{\perp} . (b) Correlation between MPD and ξ_{\perp} .

concretes and porous asphalt surfaces and calculated the mean values (MPD) and $\langle \xi_{\perp} \rangle$ for each area. The results are shown in Fig. 6(a). As can be seen a good correlation was obtained for the mean values ranging from 0.3 mm to 1.4 mm. For completeness the correlation between $\langle \text{ETD} \rangle$ and $\langle \xi_{\perp} \rangle$ is also shown in Fig. 6(b). Due to the increased statistics by means of area averaging the correlation between $\langle \text{MPD} \rangle$ and $\langle \xi_{\perp} \rangle$ is considerably improved compared to Fig. 5(b).

We conclude that this correlation can be applied in future for asphalt concrete and porous asphalt surface textures and provides a direct link between characterization of self-affine surfaces by means of the HDC and the classical surface roughness parameter ETD. It's worth mentioning that the HDC allows for the direct calculation of the ETD whereas the ETD only allows for the calculation of ξ_{\perp} , and that a direct calculation of the two other self-affine parameter ξ_{\parallel} and H is not feasible.

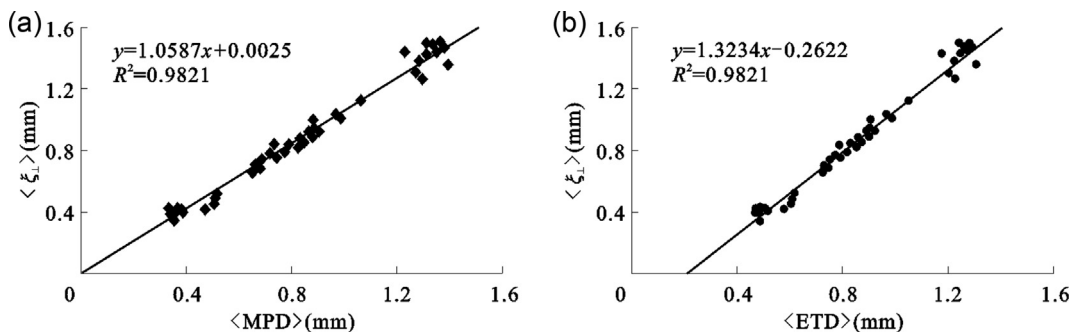


Fig. 6 – Correlation of the area averaged $\langle \xi_{\perp} \rangle$ versus $\langle \text{MPD} \rangle$ and $\langle \text{ETD} \rangle$. (a) Correlation between $\langle \xi_{\perp} \rangle$ and $\langle \text{MPD} \rangle$. (b) Correlation between $\langle \xi_{\perp} \rangle$ and $\langle \text{ETD} \rangle$.

3. Influence of pavement texture on wet skid resistance

Within this section we will discuss the interplay of pavement texture on wet skid resistance.

3.1. Influence of ETD and ξ_{\perp} on wet skid resistance

Among others tracks need to fulfill the following criteria in order to qualify as test tracks for wet braking tests within the EU tire wet grip label (European Tire and Rim Technical Organization, 2011; Kessel et al., 2013)

- The pavement should consist of dense asphalt constituting a maximum chipping size of 10 mm.
- The track's macro texture estimated by means of the sand patch method (ASTM Standard E965-96, 2006) (or ETD) must exhibit an ETD between 0.4 mm and 1.0 mm.
- The track's wet skid resistance measured by means of the so called British pendulum (ASTM Standard E303-93, 2008) must exhibit a value between 42 BPN and 60 BPN.

It is instructive to analyze whether the track's wet skid resistance measured with the British pendulum is directly related to its ETD. In Fig. 7, we present wet skid resistance pendulum measurements carried out on several kinds of pavement textures with varying ETD. From the correlation plot in Fig. 7, it is obvious that there is no direct dependency of wet skid resistance on ETD within the studied ETD levels.

The pendulum measurements are carried out on a thoroughly wetted surface area (ASTM Standard E303-93, 2008) at a slip velocity of the rubber slider of about 2.8 m/s (calculated based on the conversion of potential kinetic energy and taken into account the centre of mass of the swinging arm). Therefore some hydroplaning effects in the contact area may be expected. However, this is obviously only of minor impact for the wet skid resistance measured by the pendulum since, for example from Fig. 7, it follows that a grip level of 70 BPN is measured on asphalt concrete surfaces with an ETD between 0.5 mm and 1.0 mm. This

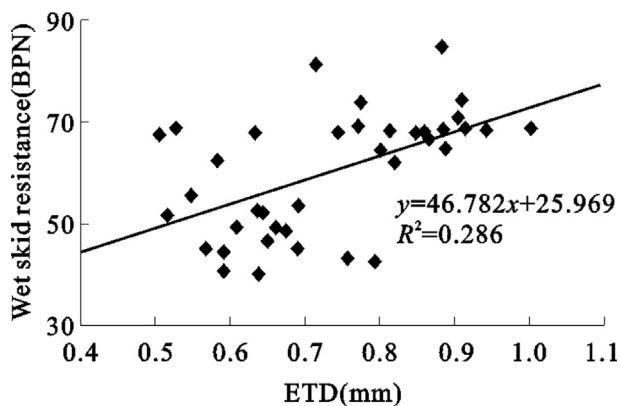


Fig. 7 – Wet skid resistance measured with the British pendulum for various asphalt concrete surfaces with varying ETD.

already covers merely the whole allowed ETD range for EU tire label wet grip test tracks.

The results of Fig. 7 reflect the fact that an estimation of the MPD or ETD is not sufficient to deduce the wet skid resistance of a pavement texture. This is in good agreement with recent studies of Bürckert et al. (2012). The reason is that MPD and ETD do not account for the microtexture of a pavement as well as the spatial distribution of surface roughness. Both have, however, a significant impact on the wet skid resistance of a pavement texture (Bürckert et al., 2012). A direct approach to access the micro texture could be the HDC function as explained previously in Section 2.

3.2. HDC as input for numerical modeling of rubber friction

Now we want to analyze whether the HDC as a complete characterization of the surface roughness on microscale and macroscale can potentially explain the relation between pavement texture and its wet skid resistance.

Neglecting other friction mechanisms like adhesion, hysteresis friction can be seen as the main contributing friction mechanism for wet grip. This important friction mechanism describes the viscoelastic energy dissipation in a deformed rubber volume due to the excitations from the surface texture. We now give a short introduction to theoretical models for hysteresis friction. More precisely, we present the main results for the calculation of hysteresis friction coefficients for a sliding rubber block on a rough asphalt surface. For more details, the reader is referred to Klüppel and Heinrich (2000) and Persson (2001).

We assume a rubber block sliding with velocity v on a rough surface with roughness given by a simple sinusoidal shape of wave length λ (Fig. 8). Then the deformation frequency ω of the rubber material is proportional to v/λ . The loss modulus or internal damping $E''(\omega)$ of the rubber material evaluated at the frequency ω of deformation can then be assumed to be proportional to the hysteresis friction coefficient. Note that the well-known elastic modulus E' as second quantity for the viscoelastic material characterization of the rubber also has an influence on hysteresis friction in the sense that it determines the contact area and the penetration depth of the rubber into the roughness of the surface. Mathematically, E' can be seen as a proportionality constant for the dependence of the loss modulus $E''(\omega)$ on hysteresis friction.

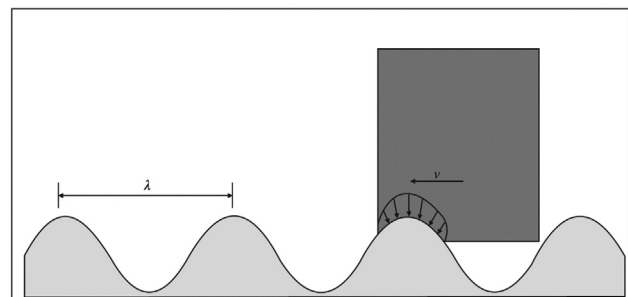


Fig. 8 – Hysteresis friction.

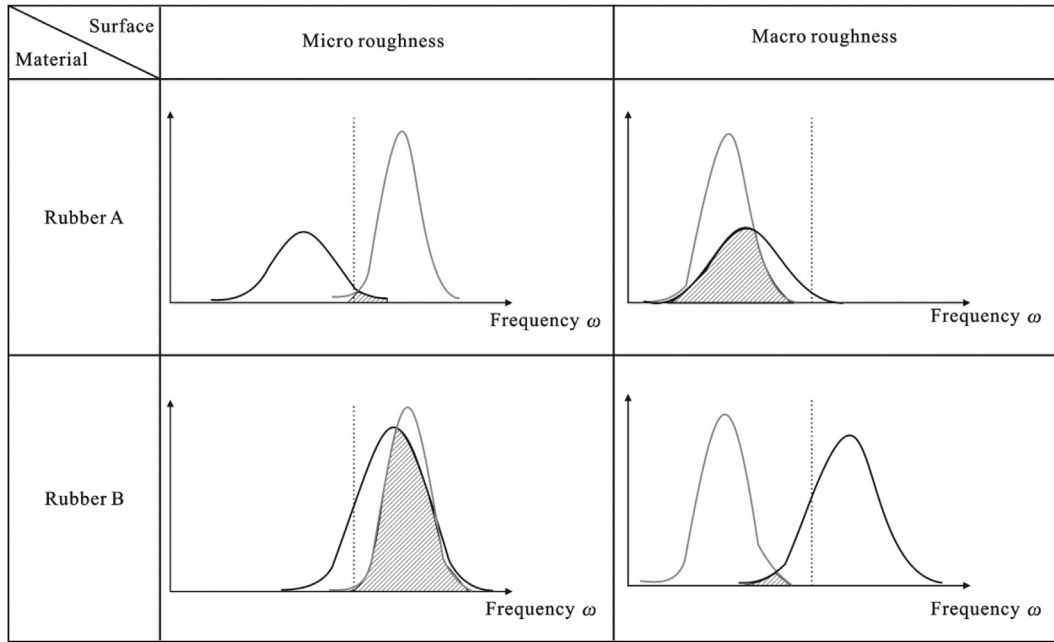


Fig. 9 – Visualization of material and surface interaction for hysteresis friction.

These straight forward arguments for the interaction of surface and material properties in case of hysteresis friction show that via the definition of the frequency ω the surface is one main influencing parameter. From material physics it is well-known that the specification of a frequency makes sense only in combination with a specified temperature T . Hence, we have to write more precisely $E''(\omega, T)$ instead of $E''(\omega)$. As a consequence, since the internal damping in general strongly depends on temperature which then also has a strong influence on hysteresis friction.

For simplicity, we assume two different rough surfaces as well as two different viscoelastic rubber materials. The two surfaces are one micro surface with main roughness on a small length and one macro surface with main roughness on a bigger length scale. Their corresponding distributions of frequencies are shown in Fig. 9 in gray color. The two rubber materials A and B are characterized by a maximal loss modulus E'' at low and high frequencies respectively indicated by black lines in Fig. 9. Extending to a frequency interval of the same physical arguments for the sinusoidal roughness with single frequency we conclude that the highest contribution to hysteresis friction is achieved for coinciding frequency distribution of the surface roughness and damping of the rubber material. More precisely, for hysteresis friction the surface texture has to excite the rubber material within a frequency interval that is characterized by significant damping. As a result we deduce again the strong influence of the surface texture and the temperature on hysteresis friction. For example, the contribution to hysteresis friction of rubber material A and B on both surfaces is visualized in Fig. 9. The higher the common area of the two curves for the surface roughness and the loss modulus the bigger is hysteresis friction.

It is clear that standard asphalt tracks do not only have micro or macro roughness but are in general a combination of

both. State of the art tire tread compounds thus perform simultaneously on all track roughness. Here, the micro and macro have just been introduced to illustrate the physical principle leading to hysteresis friction.

In the case of asphalt concrete tracks the surface roughness extends over several relevant length scales from centimeter to micrometer and the previous explanation of hysteresis friction for a simple sinusoidal roughness has to be extended. Therefore a roughness characterization over all relevant length scales is required and we introduced already the HDC as a tool for such a characterization in Section 3.1. It is immediately obvious why this kind of roughness characterization is so important for the case of rubber friction since the roughness distribution over several length scales provides directly a link to excitation spectrum within a sliding rubber block provided by the surface texture for a given sliding velocity.

The basic idea for the determination of the hysteresis friction coefficient is to calculate the dissipated energy in a volume V of the rubber material during a certain time T via the formula

$$E_d = \int_V \int_T \sigma(x, z, t) \dot{\epsilon}(x, z, t) d^2x dt \tag{11}$$

and to deduce on the friction coefficient μ_H with the help of the hysteresis force F_H given by

$$\frac{E_d}{T} = F_H v \tag{12}$$

Equation (11) can then be solved by taking the Fourier transform with respect to t and by performing the x -integration as simple multiplication. Moreover, the constitutive equations are assumed to be linear. For a given nominal pressure p and a sliding velocity v the hysteresis

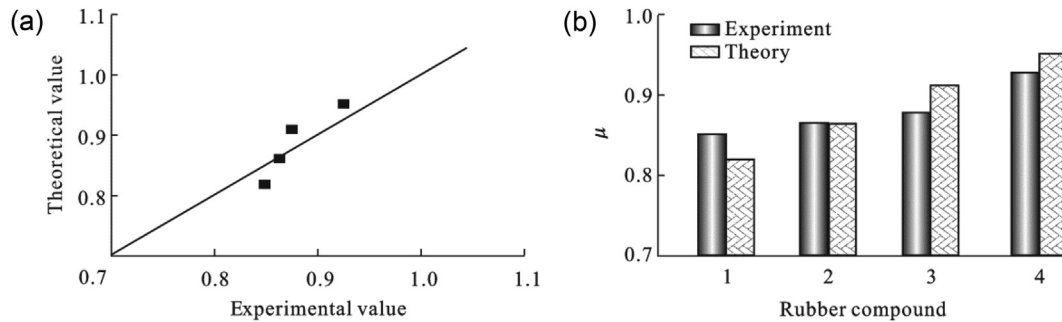


Fig. 10 – Experimental and theoretical values of friction coefficients of studied compounds (Experiments have been carried out with the LPFT at $T = 20\text{ }^{\circ}\text{C}$, $v = 1.5\text{ m/s}$, $p = 2.5\text{ bar}$). (a) Friction coefficients for several tread compounds on a wet asphalt concrete surface. (b) Experimentally measured and theoretically calculated friction coefficients of four different rubber compounds.

friction coefficient can be calculated from the following integral

$$\mu_H = \frac{1}{8\pi^2} \frac{\langle d \rangle}{pv} \int_{\omega_{\min}}^{\omega_{\max}} \omega E''(\omega) \text{PSD}(\omega) d\omega \quad (13)$$

Here the power spectrum density (PSD) is roughly speaking the Fourier transform of the height difference correlation function and the mean penetration depth $\langle d \rangle$ of the rubber into the rough surface depends on the elastic modulus E' of the rubber. Eq. (13) of the hysteresis friction coefficient is generalized to a three-dimensional theory in Persson (2001) including a length scale depending contact model. Moreover, this model can be extended by flash temperature effects (Persson, 2006). In summary, we conclude that the HDC is a suitable input parameter for the surface roughness in theoretical calculations of the wet skid resistance.

3.3. Rubber friction experiment and simulation

Finally, we want to compare the results of a friction simulation for several compounds on a wet asphalt concrete surface to experimental results. In this case the instrument of choice for the skid resistance measurement is the new developed linear portable friction tester (LPFT) device (Mihajlovic et al., 2013; Wallascheck, 2013). Note that this instrument is an alternative device to the British pendulum. This device allows to accelerate a rubber specimen in contact with the surface to a desired velocity and to measure the normal and lateral force (and hence the friction coefficient) during sliding along a track length of about 80 cm at constant velocity. Rubber samples and geometries are exchangeable within minutes. Normal load (and hence pressure p) applied onto the sample and sliding velocity v can be adjusted in order to determine the friction coefficient $\mu = \mu(p, v)$ as a function of p and v on a given track surface. This leads to a holistic characterization of the friction related properties of both rubber compound and surface.

In contrast to this, the British pendulum estimates the skid resistance of a surface by means of the totally dissipated energy due to sliding friction of the rubber slider in the contact patch. The sliding process of the pendulum, however, is

highly non-stationary and leads to a non-constant velocity of the rubber slider. The higher the skid resistance of the track the more energy is dissipated during frictional sliding and the stronger is the deceleration of the rubber slider. The pendulum gives a measure of the velocity difference between initial and final velocities of the rubber slider after the slider left the contact area. Consequently, the British pendulum with its non-constant velocity is not the instrument of choice for a comparison of measured skid resistance to the calculated friction coefficient $\mu(p, v)$.

In Fig. 10(a) we present exemplarily friction coefficient measurements obtained at $20\text{ }^{\circ}\text{C}$ on a wet asphalt concrete surface for four different rubber compounds at a velocity of 1.5 m/s and a contact pressure of 2.5 bar . Prior to the experiment the surface texture was characterized by means of a HDC function. The obtained surface parameter sets ξ_{\perp} , ξ_{\parallel} and H and the rubber characteristics $E'(\omega)$ and $E''(\omega)$ for each compound were applied in order to simulate the friction coefficients based on the methodology introduced in Section 3.2.

As a result we find a good agreement between theory and experiment. The ranking of the compounds with respect to their measured friction coefficients is well reproduced by the simulation (Fig. 10(b)).

4. Conclusions

In summary, we introduced the roughness characterization of self-affine surfaces. We conclude that both the asphalt concrete and open porous asphalt tracks exhibit self-affinity covering several length scales from micrometer to millimeter which can be visualized by the linear slope within the $\text{HDC}(\lambda)$ log–log plot. As a result of the self-affinity of asphalt tracks the surface roughness can be characterized by a set of three parameters ξ_{\perp} , ξ_{\parallel} and H . Furthermore, we demonstrate the influence of general asphalt texture feature like stone-size and spacing on these parameters. Moreover, we demonstrate that the correlation length normal to the surface ξ_{\perp} is directly related to the variance of the height distribution and provided the fact that a sufficient number of height profiles is

evaluated, and that ξ_1 is strongly correlated to entities which are typically applied for surface texture characterization in pavement engineering, namely the mean profile depths MPD and estimated texture depth ETD.

We demonstrate that both MTD and ETD do not correlate to the surface skid resistance measured with the British pendulum. We suggest instead that a surface characterization by means of $HDC(\lambda)$ over several length scales in combination with a hysteresis friction model which accounts for the properties of used rubber specimen allows theoretical estimation of the surface wet skid resistance.

From this approach together with measurements of the surface skid resistance under controlled and constant conditions (v , p , T) we can further analyze the influence of pavement texture on wet skid resistance and deduce an advanced tool box for the monitoring of our wet braking tracks used in vehicle based tire testing (Kessel et al., 2013). This approach furthermore allows a comparison of different wet skid resistance measurement techniques if all input variables like rubber specimen characteristics and testing conditions (v , p , T) are known.

REFERENCES

- ASTM Standard E965-96, 2006. Standard Test Method for Measuring Pavement Macrottexture Depth Using a Volumetric Technique. ASTM International, West Conshohocken.
- ASTM Standard E303-93, 2008. Standard Test Method for Measuring Surface Frictional Properties Using the British Pendulum Tester. ASTM International, West Conshohocken.
- Bürckert, M., Gauterin, F., Unrau, H.J., 2012. Untersuchung des Einflusses der Grobtextur auf Messergebnisse mit dem SKM-Messverfahren. Berichte der Bundesanstalt für Straßenwesen - Straßenbau Heft S 78.
- European Tire and Rim Technical Organization, 2011. Testing Method for Measuring the Wet Grip Index of C1 Tyres. UNECE Regulation No. 117, Brussels.
- ISO 13473-1:1997, 1997. Characterization of Pavement Texture by Use of Surface Profiles-part 1: Determination of Mean Profile Depth. ISO, Geneva.
- Kessel, T., Torbrügge, S., Wies, B., 2013. Vollautomatisierte Reifentests in der Halle: die Fahrbahn macht den Unterschied. In: Aachener Fahrbahnoberflächen-symposium, Aachen, 2013.
- Klüppel, M., Heinrich, G., 2000. Rubber friction on self-affine road tracks. Rubber Chemistry and Technology 73 (4), 578–606.
- Mihajlovic, S., Kuscher, U., Wies, B., et al., 2013. Methods for experimental investigations on tyre-road-grip at arbitrary roads. In: Conference Proceedings of 5th Expert Symposium on Accidental Research, Gladbach, 2013.
- Persson, B.N.J., 2001. Theory of rubber friction and contact mechanics. Journal of Chemical Physics 115, 3840–3861.
- Persson, B.N.J., 2006. Rubber friction: role of the flash temperature. Journal of Physics: Condensed Matter 18 (32), 7789–7823.
- Russ, J.C., 1994. Fractal Surfaces. Plenum Press, New York.
- Wallascheck, J., 2013. Portable linear friction tester - eine Messmethode zur objektiven Charakterisierung der Reibung im Reifen-fahrbahn-kontakt (Reifen – Fahrwerk – Fahrbahn, VDI - Berichte, Düsseldorf).